Theoretical and Mathematical Physics, **196**(2): 1150–1163 (2018)

SKYRMION STATES IN CHIRAL LIQUID CRYSTALS

G. De Matteis,* L. Martina,†‡ and V. Turco†‡

We analyze static configurations for chiral liquid crystals in the framework of the Oseen–Frank theory. In particular, we find numerical solutions for localized axisymmetric states in confined chiral liquid crystals with weak homeotropic anchoring at the boundaries. These solutions describe the distortions of two-dimensional skyrmions, known as either spherulites or cholesteric bubbles, which have been observed experimentally in these systems. We outline relations to nonlinear integrable equations and use the relations to study the asymptotic behavior of the solutions. Using analytic methods, we build approximate solutions of the equilibrium equations and analyze the generation and stabilization of these states in relation to the material parameters, external fields, and anchoring boundary conditions.

Keywords: chiral liquid crystal, weak homeotropic anchoring, skyrmion, equilibrium equation, asymptotics, nonlinear integrable equation

DOI: 10.1134/S0040577918080044

1. Introduction

Various two-dimensional structures, *cholesteric fingers*, and three-dimensional structures, *cholesteric bubbles* or *spherulites* [1], have recently been observed in thin layers of chiral liquid crystals (CLCs) with homeotropic anchoring on the confining surfaces. In particular, a phase transition between the two textures, strongly depending on the thickness of the confining cell, was detected in [2]. It was shown that the texture changes are driven by temperature through a parameter ζ proportional to the thickness and to a proper chirality parameter. Samples of different thickness displayed the textural changes at different temperatures but the same value of ζ. Pictures of the two phases obtained by polarized optical microscopy are shown in Fig. 1.

In chiral systems of this kind, these isolated axisymmetric states are stabilized by specific interactions imposed by the underlying molecular handedness [3]. In the framework of the Oseen–Frank theory, we derive the equilibrium equations for these states and study them with numerical and analytic methods.

Free states of cholesteric liquid crystals can be driven from equilibrium by applying external fields and by imposing anchoring boundary conditions [4], [5]. Experiencing both effects simultaneously, they form new structures, such as cholesteric fingers [6], [7] or helicoids with defects of the disclination type and skyrmions [8], [9], which are stabilized by topological and nontopological conservation laws and can be described in terms of integrable nonlinear equations, at least in some approximate setting [10], [11].

*Istituto di Istruzione Secondaria Superiore "V. Lilla," Francavilla Fontana (BR), Italy, e-mail: giovanni.dematteis@istruzione.it.

†Istituto Nazionale di Fisica Nucleare, Sezione di Lecce, Lecce, Italy, e-mail: martina@le.infn.it.

‡Dipartimento di Matematica e Fisica "Ennio De Giorgi," Universitá del Salento, Lecce, Italy, e-mail: vito.turco@live.com.

Prepared from an English manuscript submitted by the authors; for the Russian version, see *Teoreticheskaya i Matematicheskaya Fizika*, Vol. 196, No. 2, pp. 238–253, August, 2018.

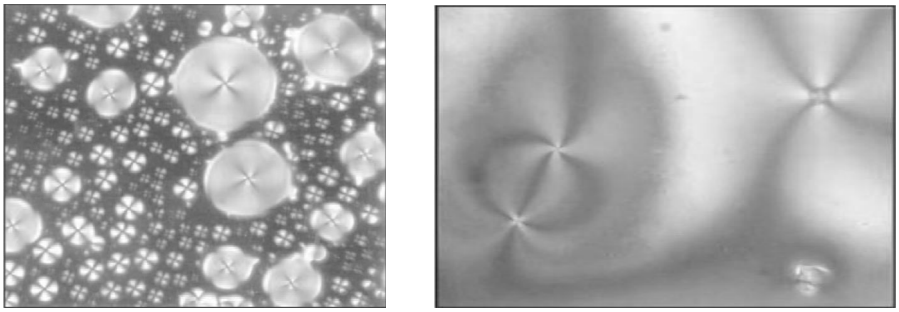

Fig. 1. Pictures of the two textures observed in chiral nematics obtained by polarized light microscopy [2].

This paper is organized as follows. In Sec. 2, after recalling the foundations of the static continuum theory for CLCs, we find and describe the skyrmion equilibrium configurations called cholesteric bubbles, mentioned above. In detail, we describe the mechanisms of their generation and stabilization, for which the anchoring boundary conditions play a crucial role. Finally, in Sec. 3, we summarize the obtained results and suggest a possible way to tackle the problem of finding analytic expressions for helicoidal equilibrium configurations in the presence of an external electric field and possible further developments of the presented analysis.

2. Skyrmions in chiral liquid crystals

We consider a static cholesteric liquid crystal confined in the region

$$\mathcal{B} = \left\{(x, y, z) \in \mathbb{R}^3 \colon |z| \le \frac{L}{2}\right\}.$$

The system is described by a unimodular director field $\mathbf{n}(\mathbf{r})$ belonging to $\mathbb{RP}^2$ (i.e., the sign of $\mathbf{n}$ is immaterial) [12], [13], which has the expression in polar representation

$$\mathbf{n}(\mathbf{r}) = (\sin\theta(\mathbf{r})\cos\psi(\mathbf{r}),\, \sin\theta(\mathbf{r})\sin\psi(\mathbf{r}),\, \cos\theta(\mathbf{r})). \tag{2.1}$$

In the bulk, the liquid crystal director field $\mathbf{n}(\mathbf{r})$ is governed by the Oseen–Frank free energy E_{FO}

$$E_{\text{FO}} = \int_{\mathcal{B}} d^3x\, \omega_{\text{FO}}[\mathbf{n}(\mathbf{x})], \tag{2.2}$$

where

$$\omega_{\text{FO}} = \frac{K_1}{2}(\nabla\cdot\mathbf{n})^2 + \frac{K_2}{2}(\mathbf{n}\cdot\nabla\times\mathbf{n} - q_0)^2 + \frac{K_3}{2}(\mathbf{n}\times\nabla\times\mathbf{n})^2 + \\ + \frac{K_2+K_4}{2}\nabla\cdot[(\mathbf{n}\cdot\nabla)\mathbf{n} - (\nabla\cdot\mathbf{n})\mathbf{n}] - \frac{\varepsilon}{2}(\mathbf{n}\cdot\mathbf{E})^2. \tag{2.3}$$

Here, q_0 is the chirality parameter of the cholesteric phase, and the positive real numbers K_1, K_2, K_3, and K_4 are the Frank elastic constants. The last term in right-hand side of (2.3) represents the interaction energy density associated with an external spatially uniform static electric field $\mathbf{E}$ along the $\mathbf{k}$ direction. Of course, in the presence of the external electric field, the general rotational symmetry is broken and reduced to rotations around the direction of $\mathbf{E}$. In the absence of anchoring conditions, the field $\mathbf{n}(\mathbf{r})$ would form

a cholesteric helix with its axis orthogonal to $\mathbf{E}$, but because of the bounding surfaces in the $\mathbf{k}$ direction, the translational symmetry in the direction of $\mathcal{B}$ is broken, and helices are hence deformed and confined within $\mathcal{B}$. Extended structures called helicoids, helicons (sometimes also called *fingers*), and spherulites (*skyrmions*) can also possibly form, depending on the existence of a preferred direction of perturbations of $\mathbf{n}$ in the directions orthogonal to $\mathbf{k}$.

To calculate the structure and energy of such perturbations, we must minimize the Frank free energy under the appropriate boundary conditions. We also consider the simplifying one-constant approximation, i.e., we set

$$K = K_1 = K_2 = K_3, \qquad K_4 = 0. \tag{2.4}$$

Expression (2.2) can then be written as

$$E_{\text{FO}} = \int d^3x \, \frac{K}{2}\biggl(|\nabla \mathbf{n}|^2 - 2q_0 \mathbf{n}\cdot\nabla\times\mathbf{n} - \frac{\varepsilon}{K}(\mathbf{n}\cdot\mathbf{E})^2\biggr), \tag{2.5}$$

where we use the well-known identity

$$(\nabla\cdot\mathbf{n})^2 + (\mathbf{n}\cdot\nabla\times\mathbf{n})^2 + (\mathbf{n}\times\nabla\times\mathbf{n})^2 + \nabla\cdot[(\mathbf{n}\cdot\nabla)\mathbf{n} - (\nabla\cdot\mathbf{n})\mathbf{n}] = |\nabla\mathbf{n}|^2.$$

Regarding the boundary conditions, we assume that there is a homeotropic anchoring. Such conditions can be encoded in a variational formulation if we consider the additional surface energy contribution

$$\omega_{\text{s}} = \frac{1}{2}K_{\text{s}}(1 + \alpha(\mathbf{n}\cdot\boldsymbol{\nu})^2), \tag{2.6}$$

where $K_{\text{s}} > 0$, $\alpha > 0$, and $\boldsymbol{\nu}$ is the unit outward normal to the boundary surface. Hence, the energy becomes $E_{\text{FO}} = \int d^3x\,(\omega_{\text{FO}} + \omega_{\text{s}})$. Such an additional term was first proposed by Rapini and Papoular in [14]. If $K_{\text{s}} \to \infty$, then we can speak of strong homeotropic anchoring, which means that the surface effects are taken into account in the form of Dirichlet boundary conditions

$$\mathbf{n}(x,y,z)|_{z=\pm L/2} = \mathbf{k} \tag{2.7}$$

without any surface-related contribution in expression (2.5) for the energy.

In what follows, we describe the mechanisms that yield skyrmionic and helicoidal perturbations when the liquid crystals are frustrated by the above geometric conditions of confinement.

We consider the director $\mathbf{n}$ in the form of Eq. (2.1). With this expression substituted in (2.5), the Oseen–Frank free-energy density functional depends on the two scalar fields $\theta(\mathbf{x})$ and $\psi(\mathbf{x})$ and their derivatives.

We limit ourself to axisymmetric isolated solutions and hence assume that $\theta = \theta(\rho, z)$ and $\psi = \psi(\phi)$, where ρ, z, and ϕ are the usual cylindrical coordinates around the axis $\mathbf{k}$. Expression (2.5) hence becomes

$$\begin{aligned} E_{\text{FO}} = \frac{K}{2}\int_0^{2\pi} d\phi \int_{-L/2}^{L/2} dz \int_0^{\infty} \rho\, d\rho \biggl[\biggl(\frac{\partial\theta}{\partial z}\biggr)^2 + \biggl(\frac{\partial\theta}{\partial\rho}\biggr)^2 + \frac{\sin^2\theta}{\rho^2}\biggl(\frac{\partial\psi}{\partial\phi}\biggr)^2 + \\ + \frac{\varepsilon E^2}{K}\sin^2\theta + 2q_0\biggl[\biggl(\frac{\partial\theta}{\partial\rho}\biggr) + \frac{\sin\theta\cos\theta}{\rho}\biggl(\frac{\partial\psi}{\partial\phi}\biggr)\biggr]\sin(\psi-\phi) + \omega_{\text{s}}(\theta)\biggr], \end{aligned} \tag{2.8}$$

where

$$\omega_{\text{s}}(\theta) = \frac{K_{\text{s}}}{K}\sin^2\theta\,\delta\biggl(z \pm \frac{L}{2}\biggr) \tag{2.9}$$

is the Rapini–Papoular energy contribution in the new coordinate system.

The Euler–Lagrange equation associated with (2.8) for ψ is

$$2\frac{\sin^2\theta}{\rho^2}\psi_{\phi\phi} - 2q_0\left[\theta_\rho + \frac{1}{2}\frac{\sin 2\theta}{\rho}\right]\cos(\psi-\phi) = 0. \tag{2.10}$$

The solution of this equation minimizing energy (2.8) is $\psi(\phi) = \phi + \pi/2$, $\phi \in [0, 2\pi]$. Substituting this equation in (2.8) yields the Euler–Lagrange equation for the field $\theta(\rho, z)$ [1]:

$$\frac{\partial^2\theta}{\partial z^2} + \frac{\partial^2\theta}{\partial\rho^2} + \frac{1}{\rho}\frac{\partial\theta}{\partial\rho} - \frac{1}{\rho^2}\sin\theta\cos\theta - \frac{2q_0}{\rho}\sin^2\theta - \frac{\varepsilon E^2}{K}\sin\theta\cos\theta = 0. \tag{2.11}$$

Because we seek finite energy solutions for $\theta \in [0, \pi]$, we impose the radial boundary conditions $\theta(\infty, z) = 0$ and $\theta(0, z) = \pi$. The alternative boundary conditions $\theta(\infty, z) = \pi$ and $\theta(0, z) = 0$ can be chosen in correspondence with the transformation $q_0 \to -q_0$ in (2.8). Indeed, the sign of q_0 determines the handedness of the configuration θ minimizing energy (2.8). We directly obtain the boundary conditions at the planar confining surfaces from $\omega_{\rm s}$ as

$$\theta_z\left(\rho, \pm\frac{L}{2}\right) = \mp\frac{K_{\rm s}}{2K}\sin 2\theta\left(\rho, \pm\frac{L}{2}\right). \tag{2.12}$$

We note that these conditions involve both θ and its derivative with respect to z.

It is convenient to rescale the equation and the boundary conditions with respect to the quantity $p = 2\pi/|q_0|$, and we thus obtain the adimensional boundary value problem

$$\frac{\partial^2\theta}{\partial z^2} + \frac{\partial^2\theta}{\partial\rho^2} + \frac{1}{\rho}\frac{\partial\theta}{\partial\rho} - \frac{1}{\rho^2}\sin\theta\cos\theta \mp \frac{4\pi}{\rho}\sin^2\theta - \pi^4\left(\frac{E}{E_0}\right)^2\sin\theta\cos\theta = 0, \tag{2.13}$$

$$\begin{aligned} &\theta(0, z) = \pi, \qquad \theta(\infty, z) = 0, \\ &\partial_z\theta\left(\rho, \pm\frac{\nu}{2}\right) = \mp 2\pi k_{\rm s}\sin\theta\left(\rho, \pm\frac{\nu}{2}\right)\cos\theta\left(\rho, \pm\frac{\nu}{2}\right), \end{aligned} \tag{2.14}$$

where $E_0 = (\pi|q_0|/2)\sqrt{K/\varepsilon}$ is the critical unwinding field for the cholesteric–nematic transition in nonconfined CLCs [15], $\nu = L/p$, and $k_{\rm s} = K_{\rm s}/Kq_0$. The sign $\pm$ in Eq. (2.13) depends on the sign of q_0. In what follows, we assume that $q_0 < 0$ with no loss of generality.

2.1. Analytic analysis of skyrmion solutions. First, we consider the radial reduction of (2.13), i.e., $\theta_z = 0$:

$$\frac{\partial^2\theta}{\partial\rho^2} + \frac{1}{\rho}\frac{\partial\theta}{\partial\rho} - \frac{1}{\rho^2}\sin\theta\cos\theta \mp \frac{4\pi}{\rho}\sin^2\theta - \pi^4\left(\frac{E}{E_0}\right)^2\sin\theta\cos\theta = 0 \tag{2.15}$$

with the boundary conditions $\theta(0) = \pi$, $\theta(\infty) = 0$. Equation (2.15) cannot be solved analytically, but we can obtain approximate analytic solutions. We note that if both $q_0 \to 0$ and $E \to 0$ in Eq. (2.15), then it reduces to the Euler–Lagrange equation of the conformally invariant $O(3)$-sigma model in the polar representation [16], i.e.,

$$\frac{\partial^2\theta}{\partial\rho^2} + \frac{1}{\rho}\frac{\partial\theta}{\partial\rho} - \frac{1}{\rho^2}\sin\theta\cos\theta = 0. \tag{2.16}$$

Solutions of this model are well known since the work of Belavin and Polyakov [17]. They are

$$\theta = \arccos\frac{\tilde\rho^2 - 4}{\tilde\rho^2 + 4}, \qquad \tilde\rho = \frac{\rho}{\rho_0}, \tag{2.17}$$

where ρ_0 is an arbitrary scale factor due to the conformal invariance.

The fourth and the fifth term in (2.15) break the conformal symmetry and thus stabilize skyrmion solutions by lowering their energy and setting the scale factor ρ_0. The two symmetry-breaking terms in fact respectively modify the Belavin–Polyakov vortex solution around $\rho = 0$ and the behavior around $\rho \to \infty$. More specifically, the external electric field affects the shape of skyrmion solutions as $\rho \to \infty$ because Eq. (2.15) in this limit reduces asymptotically to

$$\theta_{\rho\rho} - \pi^4 \left(\frac{E}{E_0}\right)^2 \sin\theta\cos\theta = 0. \tag{2.18}$$

The resulting asymptotic behavior is

$$\theta(\rho) \rightsquigarrow e^{-\rho/\rho_1} \quad \text{as} \quad \rho \rightsquigarrow \infty, \quad \text{where } \rho_1 = \frac{1}{\pi^2}\frac{E_0}{E}, \tag{2.19}$$

which shows that θ exponentially decays to zero in this limit.

To explore the behavior of the solution in a larger neighborhood of $\rho \to \infty$ and also θ around zero, we can turn to the linear approximation of Eq. (2.15), which at the first order in θ leads to the modified Bessel equation [18]

$$\rho^2 \frac{\partial^2\theta}{\partial\rho^2} + \rho\frac{\partial\theta}{\partial\rho} - \left(1 + \pi^4\left(\frac{E}{E_0}\right)^2\rho^2\right)\theta = 0. \tag{2.20}$$

Its general solution is

$$\theta(\rho) = c_1 I_1\left(\frac{\rho}{\rho_1}\right) + c_2 K_1\left(\frac{\rho}{\rho_1}\right), \tag{2.21}$$

where I_1 and K_1 are known as the first-order modified Bessel functions of the respective first and second kinds with arbitrary constants c_1 and c_2 depending on the boundary conditions.

The function K_1 has the correct asymptotic behavior as $\rho \to \infty$, but it diverges at the origin. On the other hand, $I_1(\rho/\rho_1) \to 0$ as $\rho \to 0$, but $I_1(\rho/\rho_1) \to +\infty$ as $\rho \to +\infty$, and the function I_1 therefore cannot approximate the solution we seek.

It is now clear that (2.21) cannot be an approximate solution of (2.15) for all ρ except $\rho \to \infty$ where [18] (see Eq. 8.456)

$$\theta \rightsquigarrow c_2\sqrt{\frac{\rho_1}{\rho}}e^{-\rho/\rho_1}. \tag{2.22}$$

If we now regard the interaction with the external electric field with respect to the chiral term as dominant, then we obtain a new nonlinear asymptotic approximation from Eq. (2.15),

$$\frac{\partial^2\theta}{\partial\rho^2} + \frac{1}{\rho}\frac{\partial\theta}{\partial\rho} - \frac{1}{2\rho_1^2}\sin 2\theta = 0, \tag{2.23}$$

which is known as the cylindrical sine-Gordon equation [19]. The most relevant fact about it is the connection with the celebrated Painlevé equations [20], [21]. In particular, the cylindrical sine-Gordon equation was first related to the Painlevé III equation in [22] by applying the transformation

$$\theta(\rho) = -i\log\frac{q(t)}{\sqrt{t}}, \qquad t = \left(\frac{\rho}{\rho_1}\right)^2. \tag{2.24}$$

This resulted in the equation

$$q'' = \frac{q'^2}{q} - \frac{q'}{t} + \frac{q^3}{16t^2} - \frac{1}{16q}, \tag{2.25}$$

which is a particular case of the general Painlevé III equation

$$q'' = \frac{q'^2}{q} - \frac{q'}{t} + \frac{q^2(a+cq)}{4t^2} + \frac{b}{4t} + \frac{d}{4q}, \tag{2.26}$$

where a, b, c, and d are arbitrary complex constants. Equation (2.26) was first integrated in [23], and the asymptotic forms of the solutions of this equation were analyzed in [24]. Equation (2.26) has the general solution parameterized by two complex Cauchy data, for example, α and β, such that $\theta(\rho|\alpha,\beta)$ has the asymptotic behavior

$$\theta(\rho) \rightsquigarrow \alpha \log\frac{\rho}{\rho_1} + i\frac{\pi}{2}\alpha + \beta + O\biggl(\frac{\rho}{\rho_1}\biggr)^{2-|\operatorname{Im}\alpha|} \quad (|\operatorname{Im}\alpha| < 2) \tag{2.27}$$

as $\rho \to 0$ and

$$\begin{aligned}\theta(\rho) \rightsquigarrow \biggl[b_+ e^{\rho/\rho_1}\biggl(\frac{\rho}{\rho_1}\biggr)^{-1/2+i\omega} + b_- e^{-\rho/\rho_1}\biggl(\frac{\rho}{\rho_1}\biggr)^{-1/2-i\omega}\biggr] \times \\ \times \biggl(O\biggl(\frac{\rho_1}{\rho}\biggr) + 1\biggr) + O\biggl(\biggl(\frac{\rho}{\rho_1}\biggr)^{3|\operatorname{Im}\omega|-3/2}\biggr)\end{aligned} \tag{2.28}$$

as $\rho \to \infty$, where the constants $b_\pm$ and ω are related to the Cauchy data by the *connection formulas* determined in [25] $e^{-\pi\omega}\sin(2\pi\sigma) = \sin(2\pi\eta)$ and

$$b_+ = \frac{-2^{2i\omega}e^{-\pi\omega}}{\sqrt{\pi}}\Gamma(1-i\omega)\frac{\sin(2\pi(\eta+\sigma))}{\sin(2\pi\eta)}, \qquad b_- = i\frac{2^{-2i\omega}}{\sqrt{\pi}}\Gamma(1+i\omega)\frac{\sin(2\pi(\eta-\sigma))}{\sin(2\pi\eta)}, \tag{2.29}$$

where

$$\sigma = \frac{1}{4} + \frac{i}{8}\alpha, \qquad \eta = \frac{1}{4} + \frac{1}{4\pi}(\beta + \alpha\log 8) + \frac{i}{2\pi}\log\frac{\Gamma(1/2-i\alpha/4)}{\Gamma(1/2+i\alpha/4)}. \tag{2.30}$$

These constants satisfy the relations

$$b_-b_+ = -4i\omega, \qquad |\operatorname{Im}\omega| < \frac{1}{2}. \tag{2.31}$$

Using the exponential decay of θ as $\rho \to \infty$ obtained in the linear approximation, we find that we must set $b_+ = 0$. Then $\omega = 0$ because of (2.31). Taking the other relations into account, we obtain the relation

$$\eta = -\sigma + \frac{1}{2} + k, \quad k \in \mathbb{Z}. \tag{2.32}$$

This leads to setting $b_- = -2i\sqrt{1/\pi}\cos(2\pi\sigma)$ and thus establishes a relation between α and β,

$$\beta = -\biggl(\frac{i\pi}{2} + \log 8\biggr)\alpha - 2i\log\frac{\Gamma(1/2-i\alpha/4)}{\Gamma(1/2+i\alpha/4)} + 4k\pi. \tag{2.33}$$

We should clarify that because of Eqs. (2.22), (2.29), (2.30), (2.32), and (2.33), we can obtain the value of α,

$$\alpha = -\frac{4}{\pi}\operatorname{arcsinh}\biggl(\frac{\sqrt{\pi}}{2}c_2\biggr) \in \mathbb{R}^-, \tag{2.34}$$

and the function θ as in (2.27) takes its value in $\mathbb{R}$. The irregular behavior, i.e., the logarithmic divergence as $\rho \to 0$, is a consequence of the approximation that we use to obtain Eq. (2.23) neglecting the chiral term.

Because we fail to find regular approximate solutions using standard methods, we focus on the scaling-variational ansatz in [1], [26]. Using the results obtained above, we examine this ansatz and use it to build an approximate solution of (2.13). We then study the competitive influence of the homeotropic anchoring and the external electric field on the surface.

We consider Eq. (2.15), whose solution $\theta(\rho)$ decays exponentially at large distances and behaves approximately linearly at small distances. As previously noted, the behavior around $\rho \approx 0$ is sufficiently well described by the Belavin–Polyakov solution in the form of a unit vortex. Substituting solution (2.17) in Eq. (2.15), we obtain the condition

$$-\pi^3\left(\frac{E}{E_0}\right)^2(\rho^2 - 4\rho_0^2) \mp 16\rho_0 = 0. \tag{2.35}$$

Around $\rho = 0$, it leads to an estimate of ρ_0,

$$\rho_0 = \frac{4}{\pi^3}\left(\frac{E_0}{E}\right)^2 = 4\pi\rho_1^2, \tag{2.36}$$

which can be interpreted as the typical scale of a spherulite. In this case in the vicinity of $\rho = 0$, the solution of (2.15) is approximated by the Belavin–Polyakov vortex solution with ρ_0 fixed by (2.36), which at the first order in ρ becomes

$$\theta(\rho) = \pi - \frac{\rho}{\rho_0} + O\left(\frac{\rho}{\rho_0}\right)^3. \tag{2.37}$$

For sufficiently large electric fields, i.e., $E/E_0 > 1$, around $\rho = 0$ and $\rho \to \infty$, the linear approximations match the numerical solution quite closely, as shown in Fig. 2. On the other hand, the approximations become very rough for relatively weak fields, i.e., $E/E_0 \approx 1$, as shown in Fig. 3. For the numerical cases considered here, this behavior indicates that the chiral term is underestimated in the linear approximation, in particular in the intermediate scales $\rho_1 \le \rho \le \rho_0$. Moreover, using nonlinear approximation (2.23) does not seem very helpful (at least for large electric fields). In fact, the logarithm in (2.27) pushes the region in which θ takes values near π closer to zero than Bessel K_1-type solution (2.21) does.

Seeking the z dependence of the spherulites, for our analysis, we adapt the method suggested in [1], assuming that the more relevant contribution to the free energy in Eq. (2.13) comes from a neighborhood of $\rho = 0$. In [26], it was supposed that a solution $\theta(\rho, z)$ of (2.13) is weakly modulated by a z-scaled dependence on ρ of the form

$$\theta(\rho, z) = \pi - \tilde{\theta}\left(\frac{\rho}{Z(z)}\right) \tag{2.38}$$

for a suitable $\tilde{\theta}$. In accordance with (2.37), linear approximation (2.38) must be

$$\theta(\rho, z) = \begin{cases} \pi - \dfrac{\rho}{\rho_0 Z(z)}, & 0 < \dfrac{\rho}{Z(z)} < \pi\rho_0, \\ 0, & \dfrac{\rho}{Z(z)} > \pi\rho_0, \end{cases} \tag{2.39}$$

where ρ_0 is given by (2.36).

Using Eq. (2.38), we can rewrite free energy (2.5) in units of K as

$$\overline{E} = I_0 \int_{-\nu/2}^{\nu/2} dz \left[\left(\frac{dZ}{dz}\right)^2 + A\pi^4\left(\frac{E}{E_0}\right)^2 Z^2 - B \cdot 4\pi Z + A \cdot k_s Z^2 \delta\left(z \pm \frac{L}{2}\right)\right], \tag{2.40}$$

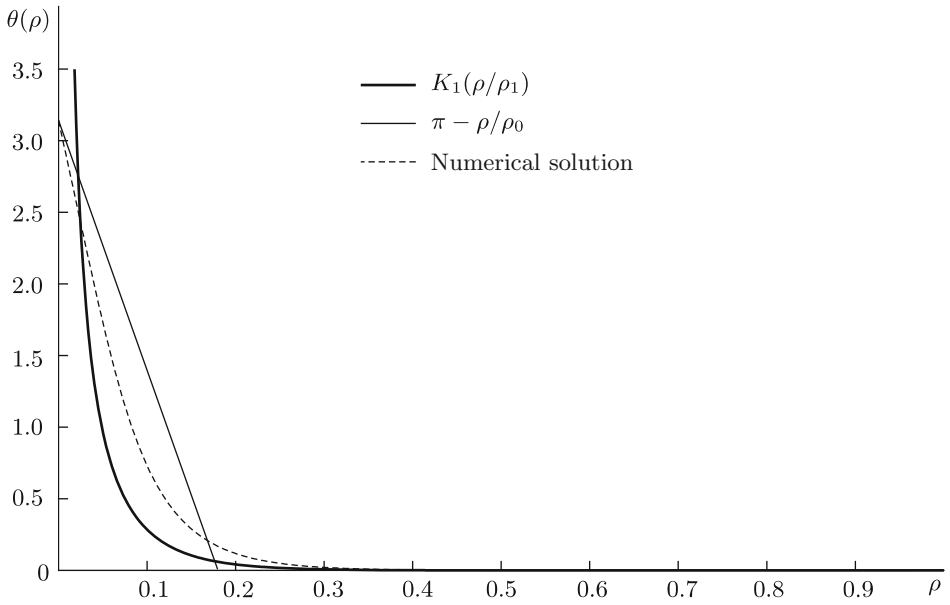

Fig. 2. Comparison of the numerical solution of (2.15) and the analytic linear approximations for $E/E_0 = 1.5$.

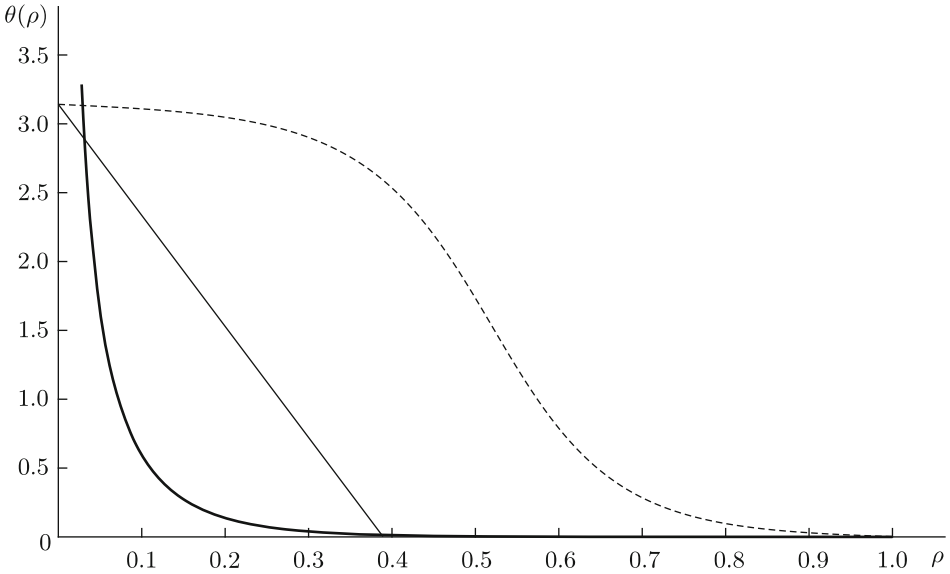

Fig. 3. Comparison of the numerical solution of (2.15) and the analytic linear approximations for $E/E_0 = 1.02$.

where

$$A = \frac{I_1}{I_0}, \qquad B = \frac{I_2}{I_0},$$

$$I_0 = \int_0^\infty \left(\frac{d\theta}{d\rho}\right)^2 \rho^3 d\rho, \qquad I_1 = \int_0^\infty \sin^2\theta\rho\, d\rho, \qquad I_2 = \int_0^\infty \left(\frac{d\theta}{d\rho} + \frac{\sin\theta\cos\theta}{\rho}\right)\rho\, d\rho,$$

and we take the conformal invariance of $(\nabla\theta)^2$ into account.

If we take expression (2.39) into account, then we can compute the integrals I_1, I_2, and I_3 explicitly

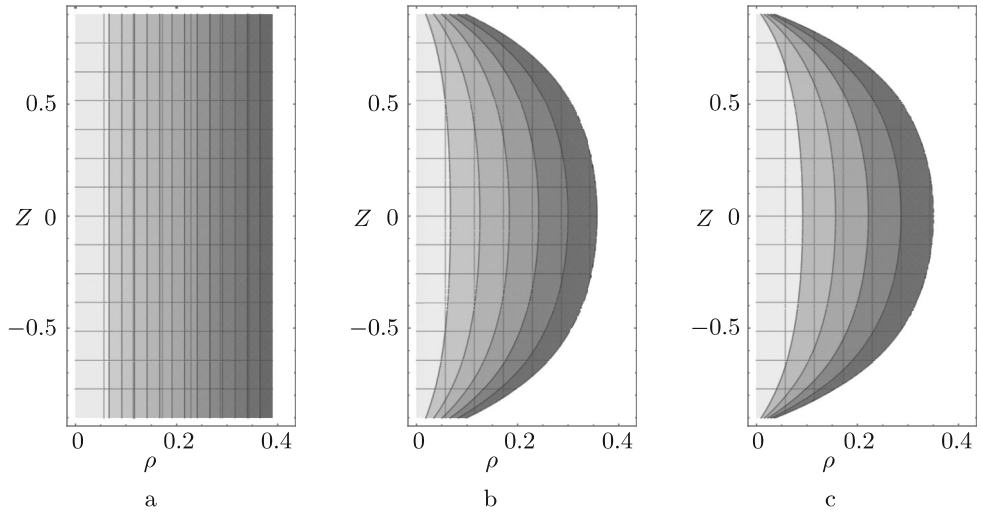

Fig. 4. Contour plot of solution (2.39) with a constant external electric field and cell thickness: the chosen parameters are $E/E_0 = 1.02$, $\nu = 1.8$, and (a) $k_\mathrm{s} = 0$, (b) $k_\mathrm{s} = 1.5$, (c) $k_\mathrm{s} = 5$.

in the interval $[0, \pi\rho_0 Z(z)]$, which yields the expression

$$\overline{E} = \frac{\pi^4}{4}\rho_1^2 (Z'(z))^2 + \frac{\pi^2}{4}(Z(z))^2 - \frac{\pi^2}{2}Z(z). \tag{2.41}$$

From this expression, we can derive the Euler–Lagrange equation for the unknown Z,

$$Z''(z) - \frac{1}{\pi^2\rho_1^2}Z(z) + \frac{1}{\pi^2\rho_1^2} = 0. \tag{2.42}$$

It has the general solution

$$Z(z) = q_1 e^{-z/(\pi\rho_1)} + q_2 e^{z/(\pi\rho_1)} + 1, \quad q_i \in \mathbb{R}. \tag{2.43}$$

Imposing boundary conditions (2.12), we obtain the approximate scaling factor

$$Z(z) = 1 - \frac{2\pi k_\mathrm{s} \cosh \frac{z}{\pi\rho_1}}{2\pi k_\mathrm{s} \cosh \frac{\nu}{2\pi\rho_1} + \frac{1}{\pi\rho_1}\sinh \frac{\nu}{2\pi\rho_1}}. \tag{2.44}$$

We note that the vortex size decreases as $|z|$ and k_s increase, as can be seen in Fig. 4.

The possibility to obtain an analytic solution, even approximate, allows studying the behavior of the skyrmion state energy. In fact, considering total energy (2.5) and substituting expressions (2.39) and (2.44) for $\theta(\rho, z)$, we obtain the estimate

$$\mathcal{E}_\mathrm{c}(E, \nu, k_\mathrm{s}) = \pi\Bigg(- \mathrm{Ci}(2\pi)\nu + \frac{32\pi^9\rho_1^3 k_\mathrm{s}^2 \sinh \frac{\rho_1\nu}{\pi}}{\left(2k_\mathrm{s}\cosh \frac{\rho_1\nu}{2\pi} + \frac{1}{\pi^2\rho_1}\sinh \frac{\rho_1\nu}{2\pi}\right)^2} - $$

$$- \frac{128\pi^9\rho_1^3 k_\mathrm{s}}{2k_\mathrm{s}\coth \frac{\rho_1\nu}{2\pi} + \frac{1}{\pi^2\rho_1}} + 24\pi^6\rho_1^2\nu + \pi^2\nu + \gamma\nu + \nu\log(2\pi)\Bigg), \tag{2.45}$$

where Ci is the cosine integral function and γ is Euler's constant.

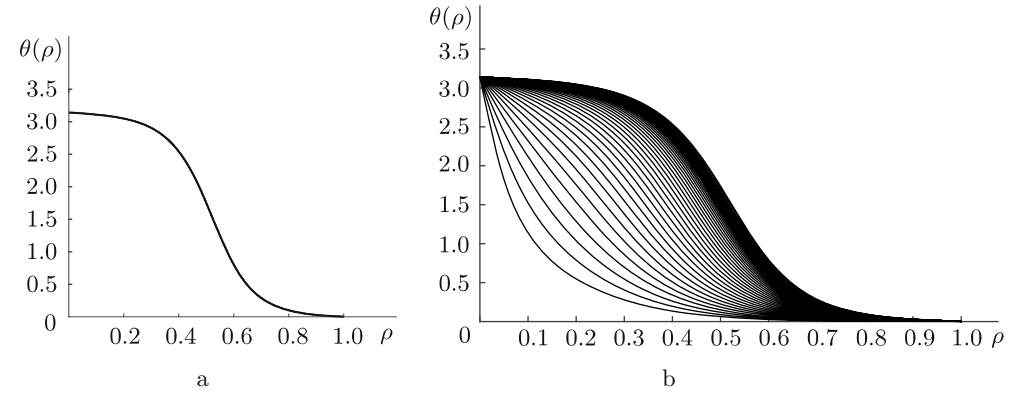

Fig. 5. Profiles of $\theta(\rho)$ for $E/E_0 = 1.02$: different curves correspond to different values of $|z|$ from $|z| = 0$ to $|z| = \nu/2$ (from right to left).

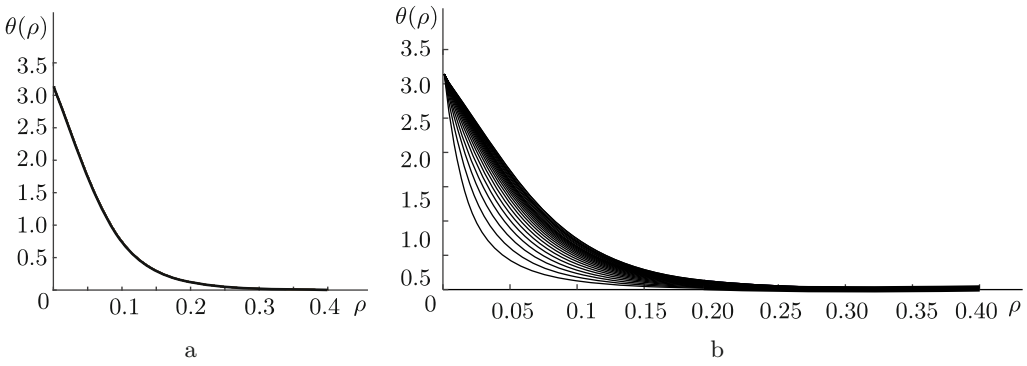

Fig. 6. The same as in Fig. 5 but for $E/E_0 = 1.5$: we note that the effect of a stronger external electric field is to reduce the vortex size for fixed values of k_{s}.

With a similar procedure, for solution (2.37) *in the bulk*, we obtain the expression for the energy

$$\mathcal{E}_{\mathrm{b}}(E,\nu) = \pi\nu\big(-\operatorname{Ci}(2\pi) + 24\pi^6\rho_1^2 + \pi^2 + \gamma + \log(2\pi)\big). \tag{2.46}$$

Clearly, with a fixed E/E_0 and ν, we have $\mathcal{E}_{\mathrm{c}} < \mathcal{E}_{\mathrm{b}}$. In particular, as k_{s} increases, the gap between the two energies increases, while it tends to decrease as E/E_0 increases, which shows the tendency to establish a uniform ordering in the liquid crystal for high values of the electric field in opposition to the chiral and anchoring effects.

2.2. Numerical analysis of skyrmion solutions. Boundary value problem (2.13) can be solved numerically by using the standard central finite-difference discretization and the Newton–Raphson method. The problem can be coded in almost any programming language [27], [28], but we used `MATLAB`[1] because it easily operates with large and sparse matrices.

To find a suitable initial guess for the iterative method, we use a shooting method for the planar reduction of Eq. (2.11) (i.e., $\theta_z = 0$) and extend the resulting planar profile over the whole cell.

The numerical solutions of boundary value problem (2.13) for different values of the pair $(E/E_0, k_{\mathrm{s}})$ are shown in Figs. 5 and 6. In each figure, the profiles $\theta(\rho)$ and shown for different values of $z \in [-\nu/2, \nu/2]$. In Fig. 5, we have $E/E_0 = 1.02$ and the anchoring strength $k_{\mathrm{s}} = 0.1$, $k_{\mathrm{s}} = 0.16$. In Fig. 6, we have $E/E_0 = 1.5$ with the same values for k_{s}. We note that if the anchoring strength is weak, then the profiles are almost

[1] `MATLAB` is a registered trademark of MathWorks, Inc., http://www.mathworks.com.

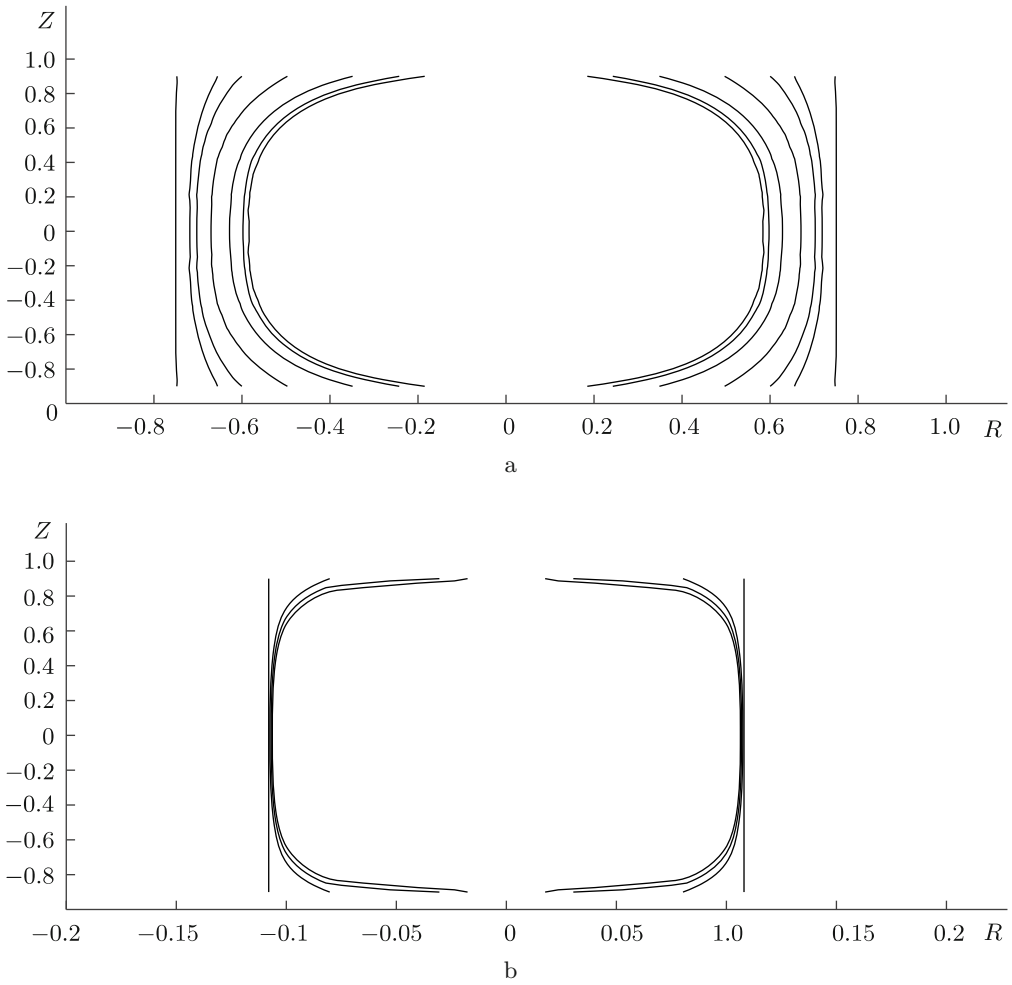

Fig. 7. Size of the planar vortices for different values of $|z|$ with the parameter $k_{\mathrm{s}} = 0.1, 0.5, 1, 1.5, 3, 6, 12$ for (a) $E/E_0 = 1.02$ and (b) $E/E_0 = 1.50$: as noted above, a quasicylindrical symmetry holds for solutions independently of the anchoring strength k_{s}, but the structures tend to the bubble form as k_{s} increases.

equal for any value of the coordinate z. This means that if the interfaces at the cell boundaries have a very small homeotropic effect on the director configuration, then a quasiperfect cylindrical symmetry holds for axisymmetric solutions. In this case, the planar vortices described by $\theta(\rho)$have the same (maximum) size for every value of z. But if we impose a quite strong homeotropic effect at the boundaries, then the vortices tend to have a reduced size, which becomes smaller as $|z|$ reaches the value $\nu/2$. In both Figs. 5 and 6, the value of the dimensionless thickness of the cell is $\nu = 1.8$.

Leonov et al. proposed a method for estimating the size of solutions of boundary value problem (2.13), similarly to what had been done for the size of ferromagnetic domain walls [1], [29]. Such a procedure consists in tracing the tangent at the inflection point $\rho_{\mathrm{I}}(z)$ of $\theta(\rho, z)$, i.e., where $\theta_{\rho\rho}(\rho_{\mathrm{I}}, z) = 0$ (numerically computed) for a fixed z. The point $R(z)$ where that tangent intersects the ρ axis gives the estimate

$$R(z) = \rho_{\mathrm{I}}(z) - \theta(\rho_{\mathrm{I}}, z)\, \theta_{\rho}(\rho_{\mathrm{I}}, z)^{-1}.$$

The results of this procedure are shown in Fig. 7 for two different values of E/E_0 considered. We stress that all vortices shrink for stronger external fields.

3. Conclusions

We have described isolated axisymmetric skyrmion states arising in confined CLCs. We showed how the interplay between chirality, external fields, and homeotropic anchoring is responsible of their generation and stabilization. The equilibrium equations for these states depend on the three material parameters E/E_0, k_s, and ν in the adimensional representation of the model introduced above.

We studied the linear approximation of Eq. (2.13) analytically. An interesting feature of such an equation is the connection, even in an approximate setting for strong electric fields, with the Painlevé III equation examined in Sec. 2. Moreover, we showed that both linear and nonlinear (in the previous sense) approximations do not take the chiral effect into account, which dominates at intermediate distances for any values of the electric field, at least below a critical value leading to the uniform distribution of the order parameter. Therefore, how to treat such a nonlinear interaction using analytic tools seems an interesting challenge for future studies.

On the other hand, using standard numerical methods, we found solutions of the model and adapted techniques from the study of magnetic domains to estimate their size and shape as functions of the material parameters mentioned above.

Finally, we compared studies of the spherulites with studies of the extended solitonic configurations in chiral nematics. In particular, an analysis of the helicoidal configurations arising in confined CLCs, cholesteric fingers, can be performed to obtain the elliptic sine-Gordon equation on the strip [1] as an equilibrium equation. Very detailed studies of the solutions of this equation are known in the literature [30], [31], generally on the whole plane or with boundary conditions significantly simpler than the homeotropic anchoring conditions, i.e., Eq. (2.7). Nevertheless, we stress that all nice solutions of the sine-Gordon equation come from its integrability properties, studied in [32], [33], where the boundary conditions enter to a large extent in defining the inverse spectral transform.

A possible reduction compatible with the above requirements is to seek solutions depending on separated x and z variables. This idea was already used several times [34]–[37] and can be implemented by the assumption $\theta = 4\arctan[X(x)Z(z)]$. Boundary conditions (2.7) yield line disclinations on the confining planes, as analyzed in [10] in the absence of external fields. Therefore, functions $X(x)$ and $Z(z)$ should be sought such that the first is monotonic and unbounded (with possible singularities at finite points) and the second takes the value $Z(\pm L/2) = \text{const}$ on the boundaries. On the other hand, more general solutions on the semistrip with suitable *integrable* boundary conditions were constructed [38], often quite implicitly. Hence, some additional work is needed to extract detailed physical information from them. The aspects just described regarding the cholesteric fingers will be presented and discussed in a future paper.

REFERENCES

1. A. O. Leonov, I. E. Dragunov, U. K. Rößler, and A. N. Bogdanov, "Theory of skyrmion states in liquid crystals," *Phys. Rev. E*, **90**, 042502 (2014).
2. C. Carboni, A. K. George, and A. Al-Lawati, "Observation of bubble domains at the cholesteric to homeotropic–nematic transition in a confined chiral nematic liquid crystal," *Liquid Crystals*, **31**, 1109–1113 (2004).
3. J. Fukuda and S. Žumer, "Quasi-two-dimensional Skyrmion lattices in a chiral nematic liquid crystal," *Nature Commun.*, **2**, 246 (2011).
4. P. Oswald and P. Pieranski, *Nematic and Cholesteric Liquid Crystals*: *Concepts and Physical Properties Illustrated by Experiments*, CRC, Boca Raton, Fla. (2005).
5. R. D. Kamien and J. V. Selinger, "Order and frustration in chiral liquid crystals," *J. Phys.*: *Condens. Matter*, **13**, R1–R22 (2001).
6. J. Baudry, S. Pirkl, and P. Oswald, "Topological properties of singular fingers in frustrated cholesteric liquid crystals," *Phys. Rev. E*, **57**, 3038–3049 (1998).

7. P. Oswald and A. Dequidt, "Thermomechanically driven spirals in a cholesteric liquid crystal," *Phys. Rev. E*, **77**, 051706 (2008).
8. T. Akahane and T. Tako, "Molecular alignment of bubble domains in cholesteric–nematic mixtures," *Japan J. Appl. Phys.*, **15**, 1559–1560 (1976).
9. B. Kerllenevich and A. Coche, "Bubble domain in cholesteric liquid crystals," *Mol. Cryst. Liq. Cryst.*, **68**, 47–55 (1981).
10. J. Fukuda and S. Žumer, "Novel defect structures in a strongly confined liquid-crystalline blue phase," *Phys. Rev. Lett.*, **104**, 017801 (2010).
11. S. Afghah and J. V. Selinger, "Theory of helicoids and skyrmions in confined cholesteric liquid crystals," *Phys. Rev. E*, **96**, 012708 (2017); arXiv:1702.06896v1 [cond-mat.soft] (2017).
12. P. D. Gennes and J. Prost, *The Physics of Liquid Crystals*, Clarendon, Oxford (1993).
13. I. W. Stewart, *The Static and Dynamic Continuum Theory of Liquid Crystals*, Taylor and Francis, London (2004).
14. A. Rapini and M. Papoular, "Distortion d'une lamelle nématique sous champ magnétique conditions d'ancrage aux parois," *J. Phys. Colloques*, **30**, No. C4, 54–56 (1969).
15. P. J. Kedney and I. W. Stewart, "On the magnetically induced cholesteric to nematic phase transition," *Lett. Math. Phys.*, **31**, 261–269 (1994).
16. N. Manton and P. Sutcliffe, *Topological Solitons*, Cambridge Univ. Press, Cambridge (2004).
17. A. A. Belavin and A. M. Polyakov, "Metastable states of two-dimensional isotropic ferromagnets," *JETP Lett.*, **22**, 245–247 (1975).
18. I. S. Gradshtein and I. M. Ryzhik, *Table of Integrals, Sums, Series, and Products* [in Russian], Fizmatgiz, Moscow (1963); English transl. *Table of Integrals, Series, and Products*, Acad. Press, New York (1980).
19. A. Barone, F. Esposito, C. J. Magee, and A. C. Scott, "Theory and applications of the sine-Gordon equation," *Riv. Nuovo Cim.*, **1**, 227–267 (1971).
20. M. J. Ablowitz and P. A. Clarkson, *Solitons, Nonlinear Evolution Equations, and Inverse Scattering* (London Math. Soc. Lect. Note Ser., Vol. 149), Cambridge Univ. Press, Cambridge (1991).
21. P. A. Clarkson, "Chapter 32 Painlevé transcendents," https://dlmf.nist.gov/32 (2018).
22. B. M. McCoy, C. A. Tracy, and T. T. Wu, "Painlevé functions of the third kind," *J. Math. Phys.*, **18**, 1058–1092 (1977).
23. A. Nakamura, "Exact cylindrical soliton solutions of the sine-Gordon equation, the sinh-Gordon equation, and the periodic Toda equation," *J. Phys. Soc. Japan*, **57**, 3309–3322 (1988).
24. A. S. Fokas, A. R. Its, A. A. Kapaev, and V. Yu. Novokshenov, *Painlevé Transcendents*: *The Riemann–Hilbert Approach* (Math. Surv. Monogr., Vol. 128), Amer. Math. Soc., Providence, R. I. (2006).
25. V. Yu. Novokshenov, "On the asymptotics of the general real-valued solution to the third Painlevé equation," *Dokl. Akad. Nauk SSSR*, **283**, 1161–1165 (1985).
26. A. N. Bogdanov, "Theory of spherulitic domains in cholesteric liquid crystals with positive dielectric anisotropy," *JETP Lett.*, **71**, 85–88 (2000).
27. W. H. Press, S. A. Teukolsky, W. T. Vetterling, and B. P. Flannery, *Numerical Recipes*: *The Art of Scientific Computing*, Cambridge Univ. Press, Cambridge (2007).
28. R. J. LeVeque, *Finite Difference Methods for Ordinary and Partial Differential Equations*: *Steady-State and Time-Dependent Problems*, SIAM, Philadelphia (2007).
29. A. Hubert and R. Schäfer, *Magnetic Domains*: *The Analysis of Magnetic Microstructures*, Springer, Berlin (2009).
30. A. B. Borisov and V. V. Kiseliev, "Topological defects in incommensurate magnetic and crystal structures and quasi-periodic solutions of the elliptic sine-Gordon equation," *Phys. D*, **31**, 49–64 (1988).
31. V. Yu. Novokshenov and A. G. Shagalov, "Bound states of the elliptic sine-Gordon equation," *Phys. D*, **106**, 81–94 (1997).
32. G. Leibbrandt, "Exact solutions of the elliptic sine equation in two space dimensions with application to the Josephson effect," *Phys. Rev. B.*, **15**, 3353–3361 (1977).

33. A. B. Borisov and V. V. Kiseliev, "Inverse problem for an elliptic sine-Gordon equation with an asymptotic behaviour of the cnoidal-wave type," *Inverse Problems*, **5**, 959–982 (1999).
34. G. L. Lamb Jr., *Elements of Soliton Theory*, Wiley, New York (1980).
35. E. L. Aero, "Plane boundary value problems for the sine-Helmholtz equation in the theory of elasticity of liquid crystals in non-uniform magnetic fields," *J. Appl. Math. Mech.*, **60**, 75–83 (1996).
36. S. V. Burylov and A. N. Zakhlevnykh, "Analytical description of 2D magnetic Freedericksz transition in a rectangular cell of a nematic liquid crystal," *Eur. Phys. J. E*, **39**, 65 (2016).
37. A. C. Bryan, C. R. Haines, and A. E. G. Stuart, "A classification of the separable solutions of the two-dimensional sine-Gordon equation and of its Laplacian variant," *Nuovo Cimento B*, **58**, 1–33 (1980).
38. A. S. Fokas, J. Lenells, and B. Pelloni, "Boundary value problems for the elliptic sine-Gordon equation in a semi-strip," *J. Nonlinear Sci.*, **23**, 241–282 (2013).